Biochimica et Biophysica Acta 934 (1988) 39–46
Elsevier

BBA 42786

Absorption spectroscopy of P-700-enriched particles isolated from spinach. Is P-700 a dimer or a monomer?

Isamu Ikegami [a] and Shigeru Itoh [b]

[a] *Laboratory of Chemistry, Faculty of Pharmaceutical Sciences, Teikyo University, Sagamiko, Kanagawa*
and [b] *National Institute for Basic Biology, Myodaiji, Okazaki (Japan)*

(Received 22 February 1988)

Key words: Photosystem I; P-700; Chlorophyll; Reaction center; (Spinach chloroplast)

A deconvolution was carried out with the low-temperature absorption spectra of P-700-enriched particles (Ikegami, I. and Katoh, S. (1975) Biochim. Biophys. Acta 376, 588–592) which had a total chlorophyll *a* (Chl *a*) to P-700 ratio of about 10. The gaussian corresponding to the reduced P-700 had a peak at 694 nm with a rather large band width. On the other hand, the gaussian corresponding to the oxidized P-700 had a peak at 687 nm with a narrow band width. The absorption spectrum of the reduced particles was fitted by the sum of five components, Chl *a*-660, Chl *a*-670, Chl *a*-675, Chl *a*-682 and Chl *a*-686 with the areas in a ratio of about 1:2 (or 3):2:2:1, in addition to Chl *a*-694 (P-700) with the area suggesting two Chl *a* in the reduced P-700. The absorption spectrum of the oxidized particles was reconstructed with the same components with almost the same stoichiometry as estimated in the reduced spectrum, except that Chl *a*-694 (P-700) was substituted to Chl *a*-687 (P-700$^+$) with the area half of the reduced P-700.

Introduction

The reaction center chlorophyll of PS I, P-700, has been proposed to be a special pair of Chl *a* molecules. This criterion is derived from the oxidized-minus-reduced difference absorption spectrum of P-700, which has a main bleaching around 700 nm with a satellite around 690 nm [1,2]. Schaffernicht and Junge [3] interpreted this spectrum on the basis of the assumption that P-700 is a dimer. A dimeric structure of P-700 was also suggested by the derivative-shaped difference circular dichroism (CD) spectrum of P-700 [4–6]. Electron paramagnetic resonance (EPR) and electron nuclear double resonance (ENDOR) data on P-700$^+$ were earlier interpreted as an evidence that the positive charge in P-700$^+$ is delocalized over two chlorophyll molecules [7,8]. However, by recent electron magnetic resonance studies, Wasielewski et al. [9,10] and O'Malley and Babcock [11] suggested that the positive charge in P-700$^+$ is located on only one chlorophyll molecule. Frank et al. [12] and Rutherford and Mullet [13] have also revealed that the EPR signal from the triplet state of P-700 was similar to that of monomeric Chl *a* triplet in vitro.

Ikegami and Katoh reported that most antenna pigments can be extracted without any loss of P-700 activity by the treatment of PS I particles with wet diethyl ether [14]. The resultant P-700-enriched particle has the total Chl *a* to P-700 ratio

---

Abbreviations: PS, Photosystem; Chl, chlorophyll.

Correspondence: I. Ikegami, Laboratory of Chemistry, Faculty of Pharmaceutical Sciences, Teikyo University, Sagamiko, Kanagawa 199-01, Japan.

as low as 8–11. Most of the Chl *a* remaining in this preparation, including P-700, might be constituents of an essential core part of the PS I reaction center, because the further enrichment of P-700 was not successful even by repeating the ether extraction [14]. Recently, we have classified these chlorophylls into several groups by a curve analysis of the room-temperature absorption spectrum, and suggested the presence of two dimer-like (Chl *a*-684, Chl *a*-674) and two monomeric (Chl *a*-669) species in addition to P-700 [15]. However, the absorption bands of the reduced and the oxidized forms of P-700 were not well characterized in that work.

In this report, we analysed the absorption spectra of P-700-enriched particles under the reduced and the oxidized conditions and estimated the absorption bands for the reduced and the oxidized state of P-700. The analysis at low temperature gave better resolution than that at room temperature, since at low temperature, the absorption spectrum of P-700-enriched particle showed a distinct shoulder around 700 nm in the presence of ascorbate or around 687 nm in the presence of ferricyanide. The absorption band estimated for the reduced P-700 had a peak at 694 nm with a rather large band width, suggesting that the number of Chl *a* involved in P-700 is 2. On the other hand, the oxidized P-700 had a peak at 687 nm with a monomer-type narrow absorption band, which suggests one Chl *a* molecule remaining unoxidized in P-700$^+$.

Materials and Methods

P-700-enriched particles were prepared as described previously [14–17]. PS-I particles, prepared by digitonin treatment of spinach chloroplasts, were lyophilized and then extracted twice with diethyl ether containing water in 80% saturation, to yield P-700-enriched particles having a Chl-*a*/P-700 ratio of about 10. The P-700-enriched particles obtained were solubilized with phosphate buffer (10 mM, pH 8) containing 0.1–0.2% Triton X-100 by incubation for 15 min at 0–4°C. Insoluble greyish-white materials were removed by centrifugation. The blue-green supernatant, which had a Chl *a* to P-700 ratio of 10, was used for measurements (cf. Ref. 17). Prior to use, it was diluted about 10-times with the same phosphate buffer without Triton X-100 to decrease detergent concentration.

The room- and low-temperature absorption and the difference-absorption spectra were determined with a Hitachi model 557 dual-wavelength spectrophotometer, as described previously [17]. Curve analysis of the absorption spectrum was carried out on a Hewlett-Packard computer (HP-9845B) with the program of Mimuro et al. [18]. P-700 was assayed from the ferricyanide (0.5 mM)-oxidized minus ascorbate (5 mM)-reduced difference spectrum, using the extinction coefficient of 64 $\mathrm{mM^{-1} \cdot cm^{-1}}$ [19]. Chlorophyll concentration was measured by the method of Arnon [20].

Results

Absorption and difference-absorption spectra of P-700-enriched particles

Fig. 1 shows the absorption spectra of P-700-enriched particles (Chl *a*/P-700 = 10) determined at 280 K (Fig. 1A) and at 90 K (Fig. 1B). At 280 K, the absorption spectrum obtained in the presence of ferricyanide (0.5 mM) (dotted line) had a peak at 675 nm with a slight shoulder around 687 nm. The addition of ascorbate (5 mM) (solid line) to the oxidized particles, induced the absorption increase both around 700 nm and 675 nm, so that the shoulder around 687 nm became less marked. At 90 K, a characteristic shoulder appeared around 700 nm in the reduced spectrum. The oxidized spectrum had no shoulder around 700 nm, but had a distinct shoulder around 687 nm, where the absorbance was slightly higher than that in the reduced spectrum. A broad peak around 675 nm at 280 K splitted into a major peak at 673 nm and a shoulder at 683 nm. Probably, the shoulder around 700 nm in the reduced spectrum reflects the absorption band of the reduced P-700, and the shoulder around 687 nm in the oxidized spectrum reflects the absorption band of the oxidized P-700 (see Fig. 3).

Fig. 2 shows the difference between the reduced and the oxidized spectra obtained at 280 K (Fig. 2A) and at 90 K (Fig. 2B). These spectra were similar to the P-700 difference spectrum already reported [1–5,21–26]. The positions of the main peak at 695 nm and of the main trough at 685 nm

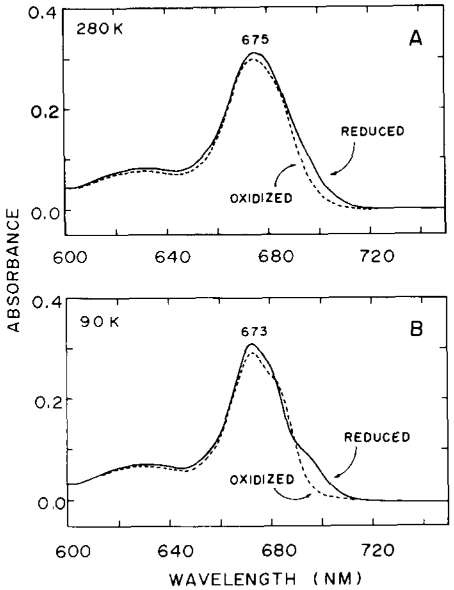

Fig. 1. Absorption spectra of P-700-enriched particles determined at 280 K (A) and 90 K (B) in the presence of 0.2 mM ferricyanide (broken lines) or in the presence of 5 mM ascorbate (solid lines). 6.0% of chlorophyll *a* in the original PS-I particles remained unextractedly in P-700-enriched particles. Chl-*a*/P-700 ratio was 10.

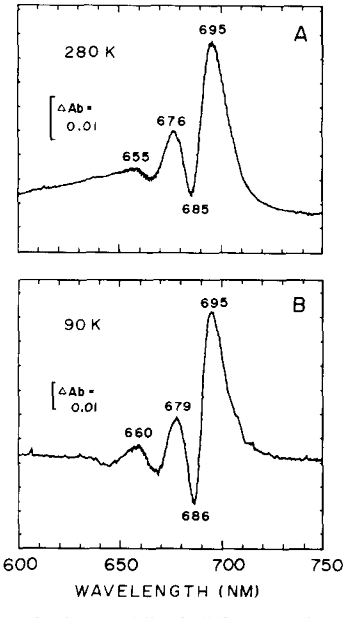

Fig. 2. Reduced-minus-oxidized difference absorption spectra of P-700-enriched particles determined at 280 K (A) and 90 K (B). Absorbance of the samples at 280 K was 0.31 at their red-band maxima. Experimental conditions were the same as in Fig. 1.

did not change so much on lowering the temperature. However, at low temperature, each band became sharper and higher. It is noted that the trough at 686 nm extended to the negative (cf. Refs. 17, 25 and 26), which reflects a higher absorbance around 687 nm in the oxidized spectrum than in the reduced one (Fig. 1B). If the difference spectrum of P-700 is mainly constructed from the two absorption bands, each corresponding to the oxidized or the reduced P-700 (cf. Refs. 3–5), the appearance of the negative peak at 686 nm at 90 K is expected as a result of narrowing of each band at low temperature.

Curve analysis on the difference-absorption spectra of P-700 at room and at low temperature

Fig. 3A shows the results on a curve analysis of the room-temperature difference spectrum. First, we estimated a gaussian corresponding to the reduced P-700, by assuming that the slope in the longer-wavelength side of the main peak in the difference spectrum reflects the slope in the absorption band of the reduced P-700, since the oxidized P-700 seems to have only a slight and flat absorption in this wavelength region [2,24]. The resultant gaussian corresponding to the reduced P-700 had a peak at 690 nm which was about 5 nm shorter than the maximum of the P-700 difference spectrum (Fig. 2A). That the absorption peak of the reduced P-700 is a little shorter than that of the difference spectrum, has already been suggested from the difference CD spectrum of P-700 [5,6,15], which had a derivative-shaped profile with a zero-crossing point at 688 nm in our preparation [15]. The estimated absorption band of the reduced P-700 had a rather large band width and covered both the main and the satellite bands in the difference spectrum. Then, we estimated another negative gaussian, so that we can construct the trough locating between the main and the satellite peak. This gaussian had a narrow band width and possibly corresponds to the absorption band of the oxidized P-700. Main features of the P-700 difference spectrum were reconstructed only with these two gaussians. This conclusion is in good agreement with the results previously obtained by Schaffernicht and Junge [3] and by Karapetyan et al. [5]. However, it was not necessary here to assume a significant contri-

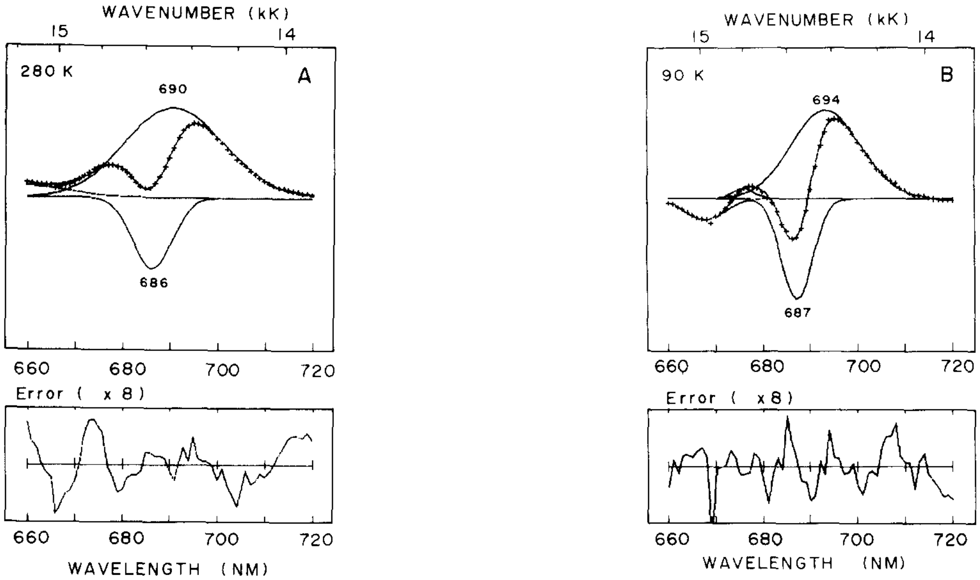

Fig. 3. Curve analysis on the difference absorption spectra of P-700-enriched particles determined at 280 K (A) and 90 K (B). The observed data are plotted as cross marks while the line through them is the sum of the component curves of which the characteristics are given in Table I. The error of fit at each point is shown below. Experimental conditions were the same as in Fig. 2.

bution of the shift-type absorption change(s) of antenna Chl *a*, probably due to the small antenna size in our preparation.

The curve analysis on the low-temperature difference spectrum (Fig. 3B) also shows that the two gaussians, each corresponding to the absorption band of the oxidized or the reduced P-700, construct the main and the satellite band, as well as the deep trough between them. We can conclude that the deeper trough around 686 nm at 90 K comes from the sharpening of each gaussian. Sétif et al. [27,28] have determined the P-700 difference spectrum at 10 K and showed a more prominent positive peak around 690 nm, suggesting a more sharpening of each absorption band at 10 K.

Table I summarizes the spectral properties of these two gaussians obtained at 280 K and 90 K. The peak position of the gaussian corresponding to the oxidized P-700 did not change so much with the change in the temperature, while the one corresponding to the reduced P-700 shifted by about 4 nm to the longer-wavelength side on lowering the temperature. This seems to be one of the reasons for the appearance of a distinct shoulder around 700 nm in the reduced absorption spectrum at low temperature (Fig. 1B). The band width of the oxidized P-700 was about half of that of the reduced P-700 (Table I). The ratio of the

TABLE I

PARAMETERS TO THE GAUSSIANS CORRESPONDING TO THE REDUCED AND THE OXIDIZED P-700

The data were taken from the results in Fig. 3.

	Peak position (nm)		Peak height (rel. unit)		Band width (1/e) (cm^{-1})		Area (rel. units)	
	280 K	90 K	280 K	90 K	280 K	90 K	280 K	90 K
Gaussians corresponding to P-700	690	694	1.00	1.00	615	429	2.00	2.00
Gaussians corresponding to P-700$^+$	686	687	−0.95	−1.14	253	198	0.83	1.06

areas over the gaussians corresponding to the oxidized and the reduced P-700 was about 1 : 2.

Curve analysis on the low-temperature absorption spectra of P-700-enriched particles

The low-temperature absorption spectrum (Fig. 1B) had a distinct shoulder around 700 nm in the reduced spectrum or around 687 nm in the oxidized spectrum, which probably reflects the absorption band of the reduced or the oxidized P-700, respectively. Fig. 4 shows the results on a curve analysis of the reduced (Fig. 4A) or the oxidized (Fig. 4B) spectrum. Table II summarizes the spectral properties to the gaussian components estimated in Fig. 4. We assumed here that the spectral properties of the oxidized and the reduced P-700 are fundamentally the same as those in Table I. We also assumed the participation of the absorption due to A_0 (the PS-I primary electron acceptor) in this wavelength region, since A_0 is suggested to be a special Chl *a* having a peak around 690 nm [29–31]. We recently determined the $A_0 - A_0^-$ difference spectrum with the P-700-enriched particles which had a narrow absorption band with a peak around 690 nm [32].

The best fit to the reduced spectrum was obtained with three major gaussians peaking at 670 nm, 675 nm and 682 nm, in addition to three minor gaussians peaking at 660 nm, 686 nm and 694 nm. The presence of the three major gaussians and one minor (Chl *a*-660) was previously suggested by a curve analysis of the room-temperature absorption spectrum [15]. Numbers of Chl *a*-660, Chl *a*-670, Chl *a*-675 and Chl *a*-682, roughly estimated with the areas over their gaussians, were about 1, 3, 2 and 2, respectively, to one P-700 (Table II). The number of Chl *a*-670 was somewhat variable between 2 and 3 in different preparations, where the lower number of Chl *a*-670 was associated with the lower Chl *a* to P-700 ratio. The shadowed component peaking at 694 nm (Fig. 4A) was introduced to reconstruct the shoulder around 700 nm in the absorption spectrum. Its characteristics presented in Table II agreed well with those to the reduced P-700 presented in Table I. The new gaussian peaking at 686 nm seems to reflect the absorption due to A_0 and had similar characteristics already estimated with the same particles by nanosecond flash photolysis [32]. The area of Chl *a*-686 was about a half of that of Chl *a*-682 or Chl *a*-675 (Table II).

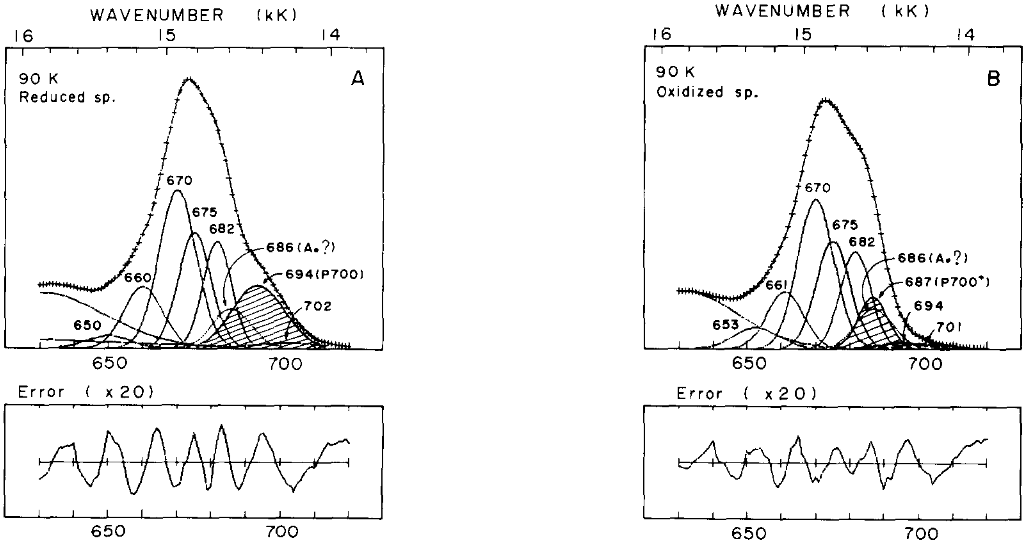

Fig. 4. Curve analysis on the absorption spectra of P-700-enriched particles determined at 90 K in the presence of 5 mM ascorbate (A) or in the presence of 0.2 mM ferricyanide (B). The observed data are plotted as cross marks while the line through them is the sum of the component curves of which characteristics are given in Table II. The error of fit at each point is shown below on a scale of 1 : 20. Experimental conditions were the same as in Fig. 1.

TABLE II

PARAMETERS TO THE GAUSSIAN COMPONENTS ESTIMATED BY A CURVE ANALYSIS ON THE LOW-TEMPERATURE ABSORPTION SPECTRA OF P-700-ENRICHED PARTICLES

The data were taken from the results in Fig. 4A and the data in parentheses from the results in Fig. 4B. The area was expressed relatively to the area over the gaussian corresponding to P-700 which was assumed as 2.0.

	Peak position (nm)	Peak height (rel. unit)	Band width (1/e) (cm^{-1})	Area (rel. unit)
Chl *b*-650	650.0	0.20	438	0.3
	(652.7)	(0.34)	(428)	(0.5)
Chl *a*-660	660.0	0.98	359	1.2
	(661.0)	(0.90)	(342)	(1.3)
Chl *a*-670	670.0	2.50	340	3.2
	(670.0)	(2.37)	(333)	(3.3)
Chl *a*-675	675.0	1.83	297	2.1
	(675.0)	(1.71)	(306)	(2.3)
Chl *a*-682	681.6	1.70	251	1.9
	(681.6)	(1.55)	(269)	(2.0)
Chl *a*-686	685.8	0.62	338	0.8
	(687.0)	(0.64)	(326)	(0.9)
Chl *a*-687	–	–	–	–
(P-700$^+$)	(686.7)	(0.83)	(254)	(0.9)
Chl *a*-694	693.5	1.00	443	2.0
(P-700)	(694.2)	(0.10)	(427)	(0.1)

A minor band at 650 nm was due to Chl *b* which was found to be present in a ratio of one or less than one molecule to one P-700 in the P-700-enriched particle [17].

The oxidized spectrum was able to be fitted by using almost the same gaussians as estimated in the reduced spectrum (Table II), only with the substitution of the spectrum of the reduced P-700 for that of the oxidized P-700. The shadowed component in Fig. 4B corresponds to the oxidized P-700, which had a peak at 687 nm with a narrow band width. Its area was about one-half of that of the reduced P-700 (Table II), in agreement with the results in Table I. The gaussian corresponding to Chl *a*-686 (A_0) almost overlapped with that of the oxidized P700 (Chl *a*-687). The slope in the longer-wavelength side was well reconstructed with these two gaussians. In order to reconstruct a small absorption still remaining around 700 nm, we assumed the gaussian corresponding to the reduced P-700 (Chl *a*-694), a part of which remained somehow unoxidized even after the chemical oxidation of P-700 (unpublished data), in addition to the gaussian to the longer wavelength-absorbing form of Chl *a* (Chl *a*-701) partially remaining unextracted after the ether treatment (cf. Ref. 33).

Discussion

In this paper, we estimated the absorption bands corresponding to the reduced and the oxidized P-700. A rather large band width of the gaussian corresponding to the reduced P-700 (Figs. 3 and 4) probably originates from a degeneration of two monomer absorption bands (cf. Refs. 3 and 5), supporting a dimeric structure of the reduced P-700. This conclusion is in good agreement with its derivative-shaped CD signal [15]. The dimeric nature of P-700 has been also suggested by the recent photochemical hole-burning experiments for P-700 [34].

Sétif et al. [27] and Den Blanken and Hoff [35] have recently determined the triplet-minus-singlet spectrum of P-700 at liquid helium temperature, which was different from the oxidized-minus-reduced difference spectrum of P-700 with respect to a smaller contribution of a positive peak around 685 nm in the former spectrum. Consequently, the triplet-minus-singlet spectrum of P-700 may reflect the absorption band of the reduced P-700 more directly, because the triplet state of P-700, unlike P-700$^+$, probably has not a significant absorption in the red-band region. We recently studied the triplet-minus-singlet spectrum of P-700 at 280 K and 110 K in order to obtain a more direct evidence for the spectral feature of the reduced P-700 (Itoh, S., Iwaki, M. and Ikegami, I., unpublished data). The triplet-minus-singlet spectrum of P-700 studied had also a rather large band width at room temperature. It became narrower on lowering the temperature with the red shift of the absorption maximum (cf. Table I). The reason why the absorption of the reduced P-700 shifts to the longer-wavelength side on lowering the temperature is not clear now.

The integral over the absorption band of the oxidized P-700 corresponded to about one-half of that of the reduced P-700 (Tables I and II). In addition, it has a narrow absorption band (Fig. 4B). These observations suggest a monomeric structure of the oxidized P-700, and support the previous interpretation [36,37] that the positive charge on the oxidized P-700 is localized on only one of the two Chl *a* molecules in P-700. Thus, we can ascribe the absorption of P-700^+ to the weakly coupled reduced partner of the dimer (cf. Ref. 35), whereas the oxidized partner has no absorption around the red-band region. This may be the reason for the previous proposals that P-700 is a monomeric Chl *a* [9–13] because these proposals have been introduced from the experiments on the oxidized form of P-700 (cf. Ref. 35–37).

Several Chl *a* derivatives (*enol* form, Chl *a*′, Chl RC-I) have been proposed as the chemical identity of P-700 [10,38,39]. Recently, we have analysed the Chl *a* in P-700-enriched particle by high-performance liquid chromatography [40] and found that a Chl *a*′ presents in a molar ratio of 1 : 1 P-700. This suggests a close location of Chl *a*′ to the core site of the PS-I reaction center. However, the results exclude the possibility that P-700 consists of a dimer of Chl *a*′. The location and function of the Chl *a*′ will be a problem in future.

Our PS-I particle used here had only 10 Chl *a* to one reaction-center unit. We could assign two of them to the constituents of P-700. Other Chl have been classified into several components by a curve analysis of the low-temperature absorption spectra (Fig. 4, Table II) (cf. Ref. 15). The number of Chl *a* included in each of these species could be roughly estimated, in comparison with the integral over the gaussian of each component, at one in Chl *a*-660, two (or three) in Chl *a*-670, two in Chl *a*-675, two in Chl *a*-682 and one in Chl *a*-686, in addition to two in P-700, which sums up to ten (or eleven) Chl *a* to one reaction-center unit (cf. Table II). Chl *a*-682, another dimeric species in P-700-enriched particles, probably acts as the closest antenna to P-700, since the action spectrum to the PS-I variable fluorescence, which seems to be the delayed fluorescence induced by the charge recombination of the radical pair (P-700^+-A_0^-) [41] (Mimuro, M., et al., unpublished data), suggests an efficient energy transfer from this chlorophyll to P-700 [16]. Two Chl *a*-675 molecules have a CD-active organization [16]. However, this chlorophyll shows a low efficiency of its energy transfer to P-700 [41] (Mimuro, M., et al., unpublished data).

The PS-I primary electron acceptor, A_0, is suggested to be a Chl *a* species (cf. Refs. 36 and 37). We have now two candidates for A_0 in literature, i.e., Chl *a*-670 and Chl *a*-690. The photoaccumulation technique firstly employed for the detection of EPR signal of A_0 [42] reveals that A_0 may be a Chl *a* monomer with an absorption peak around 670 nm (Chl *a*-670) [17,43,44]. In contrast, the more recent results obtained by the picosecond laser photolysis suggest that A_0 has an absorption around 690 nm (Chl *a*-690) [29–31]. We are able to identify either of these two species (Chl *a*-670 and Chl *a*-690 (686)) by the curve analysis of the P-700-enriched particle as shown in Fig. 4. The relationship between these two species is still unclear. Recently, we determined the A_0/A_0^- difference spectrum by nanosecond flash photolysis with the P-700-enriched particles, which lack all the vitamin K-1 and showed, after a laser flash, the nanosecond decay of P-700^+ probably due to the back electron flow from A_0^- [32,45,46]. The spectrum showed a single and narrow bleaching around 690 nm, without any appreciable shoulder around 670 nm [32]. Moreover, we observed no derivative-shaped CD signal originating from Chl *a*-690 (A_0) in our preparation [15]. These results suggest that Chl *a*-690 is a monomeric Chl *a* and acts as a primary electron acceptor of PS-I. Fluorescence studies suggest that Chl *a*-670 is an efficient antenna to P-700 [17,41]. Probably Chl *a*-670 locates very close to the primary acceptor A_0 (Chl *a*-690), and may be reduced via A_0 under the strongly reducing conditions.

Acknowledgements

We thank Drs. M. Mimuro and Y. Fujita (National Institute for Basic Biology (NIBB)) for generously allowing us the use of their curve analysis program and for their valuable discussions. This work was supported in part by grants from the Ministry of Education, Science and Culture in Japan, and by Co-operative Research Program of NIBB in Japan.

References

1 Kok, B. (1957) Acta Bot. Neerl. 6, 316–337.
2 Ke, B. (1972) Arch. Biochem. Biophys. 152, 70–77.
3 Schaffernicht, H. and Junge, W. (1981) Photochem. Photobiol. 34, 223-232.
4 Philipson, K.D., Sato, V.L. and Sauer, K. (1972) Biochemistry 11, 4591–4595.
5 Shubin, V.V., Efimovskaya, T.V. and Karapetyan, N.V. (1981) J. Phys. Chem. (Sov.) 55, 2916–2921.
6 Karapetyan, N.V., Shubin, V.V., Rakhimberdieva, M.G., Vashchenko, R.G. and Bolychevtseva, Y.V. (1984) FEBS Lett. 173, 209-212.
7 Norris, J.R., Uphaus, R.A., Crespi, H.L. and Katz, J.J. (1971) Proc. Natl. Acad. Sci. USA 68, 625-628.
8 Norris, J.R., Scheer, H., Druyan, M.E. and Katz, J.J. (1974) Proc. Natl. Acad. Sci. USA 77, 4897-4900.
9 Wasielewski, M.R., Norris, J.R., Shipman, L.L., Lin, C.-P. and Svec, W.A. (1981) Proc. Natl. Acad. Sci. USA 78, 2957–2961.
10 Wasielewski, M.R., Norris, J.R., Crepsi, H.L. and Harper, J. (1981) J. Am. Chem. Soc. 103, 7664-7665.
11 O'Malley, P.J. and Babcock, G.T. (1984) Proc. Natl. Acad. Sci. USA 81, 1098-1101.
12 Frank, H.A., McLean, M.B. and Sauer, K. (1979) Proc. Natl. Acad. Sci. USA 76, 5124-5128.
13 Rutherford, A.W. and Mullet, J.E. (1981) Biochim. Biophys. Acta 635, 225-235.
14 Ikegami, I. and Katoh, S. (1975) Biochim. Biophys. Acta 376, 588-592.
15 Ikegami, I. and Itoh, S. (1986) Biochim. Biophys. Acta 851, 75-85.
16 Ikegami, I. (1976) Biochim. Biophys. Acta 449, 245-258.
17 Ikegami, I. and Ke, B. (1984) Biochim. Biophys. Acta 764, 70-79.
18 Mimuro, M., Murakami, A. and Fujita, Y. (1982) Arch. Biochem. Biophys. 215, 266-273.
19 Hiyama, T. and Ke, B. (1972) Biochim. Biophys. Acta 267, 160-171.
20 Arnon, D.I. (1949) Plant Physiol. 24, 1-15.
21 O'Reilly, J.E. (1973) Biochim. Biophys. Acta 292, 509-515.
22 Shuvalov, V.A., Dolan, E. and Ke, B. (1979) Proc. Natl. Acad. Sci. USA 76, 770-773.
23 Doering, G., Bailey, J.L., Kreutz, W., Weikard, J. and Witt, H.T. (1968) Naturwissenschaften 55, 219-220.
24 Inoue, Y., Ogawa, T. and Shibata, K. (1973) Biochim. Biophys. Acta 305, 483-487.
25 Lozier, R.H. and Butler, W.L. (1974) Biochim. Biophys. Acta 333, 465-480.
26 Verméglio, A., Breton, J. and Mathis, P. (1976) J. Supramol. Struct. 5, 109-117.
27 Sétif, P., Hervo, G. and Mathis, P. (1981) Biochim. Biophys. Acta 638, 257-267.
28 Sétif, P., Mathis, P. and Vänngård, T. (1984) Biochim. Biophys. Acta 767, 404-414.
29 Nuijs, A.M., Shuvalov, V.A., Van Gorkom, H.J., Plijter, J.J. and Duysens, L.N.M. (1986) Biochim. Biophys. Acta 850, 310-318.
30 Shuvalov, V.A., Nuijs, A.M., Van Gorkam, H.J., Smit, H.W.J. and Duysens, L.N.M. (1986) Biochim. Biophys. Acta 850, 319-323.
31 Wasielewski, M.R., Fenton, J.M. and Govindjee (1987) Photosynth. Res. 12, 181-190.
32 Mathis, P., Ikegami, I. and Sétif, P. (1988) Photosynth. Res., in press.
33 Ikegami, I. (1983) Biochim. Biophys. Acta 722, 492-497.
34 Gillie, J.K., Fearey, B.L., Hayes, J.M., Small, G.J. and Golbeck, J.H. (1987) Chem. Phys. Lett. 134, 316-322.
35 Den Blanken, H.J. and Hoff, A.J. (1983) Biochim. Biophys. Acta 724, 52-61.
36 Rutherford, A.W. and Heathcote, P. (1985) Photosynth. Res. 9, 295-316.
37 Sétif, P. and Mathis, P. (1986) in Encyclopedia of Plant Physiology (Staehelin, L.A. and Arntzen, C.J., eds.), New Series, Vol. 19, Photosynthesis III, pp. 476-486, Springer-Verlag, Berlin.
38 Watanabe, T., Kobayashi, M., Hongu, A., Nakazato, M., Hiyama, T. and Murata, N. (1985) FEBS Lett. 191, 252-256.
39 Donemann, D. and Senger, H. (1986) Photochem. Photobiol. 43, 573-581.
40 Watanabe, T., Kobayashi, M., Nakazato, M., Ikegami, I. and Hiyama, T. (1987) in Progress in Photosynthesis Research (Biggins, J., ed.), Vol. I, pp. 303-306, Martinus Nijhof, Dordrecht.
41 Ikegami, I. and Ke, B. (1984) Biochim. Biophys. Acta 764, 80-85.
42 Bonnerjea, J. and Evans, M.C.W. (1982) FEBS Lett. 148, 313-316.
43 Swarthoff, T., Gast, P., Amesz, J. and Buisman, H.P. (1982) FEBS Lett. 146, 129-132.
44 Mansfield, R.W. and Evans, M.C.W. (1985) FEBS Lett. 190, 237-241.
45 Itoh, S., Iwaki, M. and Ikegami, I. (1987) Biochim. Biophys. Acta 893, 508-516.
46 Ikegami, I., Sétif, P. and Mathis, P. (1987) Biochim. Biophys. Acta 894, 414-422.